Journal of Experimental Botany, Vol. 64, No. 12, pp. 3869–3884, 2013
doi:10.1093/jxb/ert218
This paper is available online free of all access charges (see http://jxb.oxfordjournals.org/open_access.html for further details)

Journal of Experimental Botany
www.jxb.oxfordjournals.org

RESEARCH PAPER

Virus-induced gene silencing unravels multiple transcription factors involved in floral growth and development in *Phalaenopsis* orchids

Ming-Hsien Hsieh[1,2], Zhao-Jun Pan[1], Pei-Han Lai[1], Hsiang-Chia Lu[3], Hsin-Hung Yeh[3], Chia-Chi Hsu[1], Wan-Lin Wu[4], Mei-Chu Chung[5], Shyh-Shyan Wang[2], Wen-Huei Chen[6] and Hong-Hwa Chen[1,4,6,*]

[1] Department of Life Sciences, National Cheng Kung University, Tainan 701, Taiwan
[2] Tainan District Agricultural Research and Extension Station, Council of Agriculture, Tainan 712 Taiwan
[3] Department of Plant Pathology and Microbiology, National Taiwan University, Taipei 106, Taiwan
[4] Institute of Tropical Plant Sciences, National Cheng Kung University, Tainan 701, Taiwan
[5] Institute of Plant and Microbial Biology, Academia Sinica, Taipei 115, Taiwan
[6] Orchid Research Center, National Cheng Kung University, Tainan 701, Taiwan

* To whom correspondence should be addressed. E-mail: hhchen@mail.ncku.edu.tw

Received 13 May 2013; Revised 11 June 2013; Accepted 18 June 2013

Abstract

Orchidaceae, one of the largest angiosperm families, has significant commercial value. Isolation of genes involved in orchid floral development and morphogenesis, scent production, and colouration will advance knowledge of orchid flower formation and facilitate breeding new varieties to increase the commercial value. With high-throughput virus-induced gene silencing (VIGS), this study identified five transcription factors involved in various aspects of flower morphogenesis in the orchid *Phalaenopsis equestris*. These genes are *PeMADS1*, *PeMADS7*, *PeHB*, *PebHLH*, and *PeZIP*. Silencing *PeMADS1* and *PebHLH* resulted in reduced flower size together with a pelaloid column containing petal-like epidermal cells and alterations of epidermal cell arrangement in lip lateral lobes, respectively. Silencing *PeMADS7*, *PeHB*, and *PeZIP* alone resulted in abortion of the first three fully developed flower buds of an inflorescence, which indicates the roles of the genes in late flower development. Furthermore, double silencing *PeMADS1* and *PeMADS6*, C- and B-class MADS-box genes, respectively, produced a combinatorial phenotype with two genes cloned in separate vectors. Both *PeMADS1* and *PeMADS6* are required to ensure the normal development of the lip and column as well as the cuticle formation on the floral epidermal cell surface. Thus, VIGS allows for unravelling the interaction between two classes of MADS transcription factors for dictating orchid floral morphogenesis.

Key words: *Cymbidium* mosaic virus, *PebHLH*, *PeMADS1*, *PeMADS6*, *Phalaenopsis*, virus-induced gene silencing.

Introduction

The Orchidaceae, well known for fascinating flowers, is one of the largest and most diverse families of flowering plants. The family contains more than 25 000 species that occupy wide ranges of ecological habitats and exhibit highly specialized morphological, structural, and physiological characteristics (Dressler, 2005). The orchid flowers of the species usually have two lateral petals with a third larger petal modified into a lip to attract and in some cases trap potential pollinators. The column contains the male stamens attached to the female pistil in the centre. Because of their unique flowers, orchid reproductive biology is of special interest in terms of flower colour, flower morphological features, size and number of flowers, and floral fragrance (Hsiao *et al.*, 2011).

The orchid industry has become an international business, comprising approximately 8% of the world's floriculture

trade (Chugh *et al.*, 2009). In particular, *Phalaenopsis* and *Oncidium* are the cash crops. The identification and analysis of orchid gene functions could help improve orchids in terms of flower shape, size, scent, and colouration. Such investigation helps understand orchid biology and enhances the breeding of new varieties to increase the commercial value. These traits need to be studied to have a better understanding of the genetic factors and how morphological traits are determined in the orchid flower. However, the challenges are the lack of information on the genetic background of various cultivars, large genome size, long life cycle, and the inefficient transformation system of orchids. The study of functional genomics of orchid genes is difficult and inefficient.

Virus-induced gene silencing (VIGS) is a reverse genetics approach used for functional analysis of genes of plants, especially those with long life cycles and few genetic resources such as orchids. The technique has many advantages over other techniques used for functional analysis, such as cost-effectiveness with the use of expressed sequence tags (ESTs), good for orchid research because whole-genome sequences are not yet available. The analyses of floral bud ESTs in the OrchidBase (http://orchidbase.itps.ncku.edu.tw/est/home2012.aspx) have been initiated for *Phalaenopsis aphrodite* subsp. *formosana*, *Phalaenopsis bellina*, and *Phalaenopsis equestris*, which are usually used as parents for breeding (Hsiao *et al.*, 2006; Tsai *et al.*, 2006, 2013; Fu *et al.*, 2011). A *Cymbidium* mosaic virus (CymMV)-based VIGS vector has been established (Lu *et al.*, 2007) and was used to determine the effects of *PeUFGT3* on anthocyanin biosynthesis (Chen *et al.*, 2011), *PeMADS5* and *PeMADS6* on floral morphogenesis (Hsieh *et al.*, 2013), and *PhaTF15* on disease resistance in *Phalaenopsis* (Lu *et al.*, 2012).

Several functional studies of floral transcription factors (TFs) have revealed their critical roles in a number of developmental processes in orchid plants. The MADS-box gene family encodes highly conserved TFs. The floral MADS-box genes of *Arabidopsis* have been divided into several major classes (A, B, C, D, and E) by phylogenetic analysis (Becker and Theissen, 2003); the function of ABCDE genes is partially conserved between *Arabidopsis* and orchid (Xu *et al.*, 2006; Tsai *et al.*, 2010; Xu *et al.*, 2010). From the ABCDE model in *Phalaenopsis*, *PeMADS1* is a C-class *AGAMOUS*-like MADS-box gene involved in the development of reproductive organs (Song *et al.*, 2006; Chen *et al.*, 2012), and *PeMADS6* is a B-class *GLOBOSA*/*PISTILLATA*-like MADS-box gene ubiquitously expressed in the sepals, petals, lip, and column (Tsai *et al.*, 2005). Silencing *PeMADS6* confers leaf-like characteristics with greenish and discoloured areas in sepals, petals, and lip (Lu *et al.*, 2007; Hsieh *et al.*, 2013). *PeMADS7* is a D-class gene that plays important roles in column and ovule development in *Phalaenopsis* (Chen *et al.*, 2012). Except for MADS-box genes, little is known about the functions of floral TFs in orchids as compared with those involved in floral development in *Arabidopsis*.

To understand individual TFs that affect orchid floral morphogenesis and development, this study used high-throughput VIGS to silence the expression of 126 floral ESTs that encode TFs and examined their functions during floral morphogenesis in *Phalaenopsis*. The high-throughput VIGS process involves cloning libraries of short gene fragments, such as ESTs, directly into a VIGS vector, inoculating plants, and then identifying phenotypes of interest (Bernacki *et al.*, 2010; Lu *et al.*, 2012). Moreover, this work studied the cooperative action of different classes of MADS-box TFs by co-silencing with separate VIGS vectors. This process helped to unravel the functions of TFs involved in orchid floral morphogenesis.

Materials and methods

Plant materials

The *Phalaenopsis* plants purchased from Oxen Biotechnology (Tainan, Taiwan) were *Doritaenopsis* I-Hsin Sunrise Cinderella 'OX1357', *Dtps*. OX Red Shoe 'OX1407', and *Phalaenopsis* Sogo Yukidian 'V3'. All plants were kept in a greenhouse with a controlled temperature of 27/22 °C (day/night). Plants were determined to be virus-free by reverse-transcription (RT)-PCR with two primer pairs, CymMV-CPF/CymMV-CPR and ORSV-CPF/ORSV-CPR (Supplementary Table S1, available at *JXB* online), for detecting the two prevalent orchid viruses, CymMV and ORSV, respectively, before VIGS experiments.

Construction of pCymMV-Gateway plasmids

The putative TFs of 152 ESTs were identified from 5593 orchid floral ESTs in the *Arabidopsis thaliana* TF database at the *Arabidopsis* Gene Regulatory Information Server (AGRIS) (http://arabidopsis.med.ohio-state.edu) (Tsai *et al.*, 2006). Each EST was then cloned into pBluescript SK+ plasmid. Clones underwent PCR amplification with the primers for AttB1 (5′-GGGGACAAGTTTGTACAAAAAAGCAGGCTGCTC TAGAACTAGTGGATCCCCCG-3′) and AttB2 (5′-GGGGACC ACTTTGTACAAGAAAGCTGGGTGCGAATTGG GTACCGGGCCCCCCC-3′). The length of EST sequences ranged from 0.5 to 3.3 kb (Supplementary Fig. S1). The amplified PCR products were purified with use of polyethylene glycol/$MgCl_2$ to remove primers. Purified PCR products were recombined into the pCymMV-Gateway vector by use of BP recombinase (Invitrogen, Carlsbad, CA, USA). As a result, only 126 ESTs were successfully cloned into the pCymMV-Gateway vector. After recombination into the pCymMV-Gateway vector, each construct was confirmed by PCR with the primer pairs for AttB1 and CymMV-5351 (5′-CTTCTGTACCATACACATAG-3′).

Agro-infiltration of plants

Agrobacterium tumefaciens containing the pCymMV-Gateway-EST was cultured overnight at 28 °C. After centrifugation, bacterial cell pellets were resuspended by adding 300 µl Murishige and Skoog medium containing 100 µM acetosyringone to OD_{600} = 1 and allowed to stand at room temperature for 0.5 h without shaking before agro-infiltration. Then plants were infected following the standard protocol established previously (Hsieh *et al.*, 2013). The suspensions were injected into the leaf right above the inflorescence emerging site by use of a 1-ml syringe with a needle. Plants with inflorescences containing eight nodes with one visible floral bud were inoculated (Supplementary Fig. S2D).

This work silenced 126 TF ESTs and one control, *PeMADS6* (GenBank AY678299.1). For quantification of agro-infiltration to determine efficacy, the positive control plants were infiltrated with a pCymMV-Gateway vector inserted with a fragment of *PeMADS6* cDNA, which showed morphological changes with greenish and discoloured areas in the sepal, petal and lip (Hsieh *et al.*, 2013).

Mock-treated plants were injected with an empty pCymMV-Gateway vector as a negative control to confirm that floral morphogenesis was not due to the viral infection. Each experiment involved five plants, and the silencing experiments for TFs with distinctive phenotypes on silencing were repeated at least twice in different cultivars. The TFs included *PeMADS1* (GenBank AF234617.1), *PeMADS7* (GenBank JN983500.1), *PebHLH* (OrchidBase 2.0 lcl|EFCPTF-001B04-02B1), *PebZIP* (OrchidBase 2.0 lcl|Unigene59946_Pe_fb), and *PeHB* (OrchidBase 2.0 lcl|AECP-22H12 AECP-22H12) (Fu *et al.*, 2011; Tsai *et al.*, 2013). The total number of inoculated plants and replicates from each treatment group are in Supplementary Tables S2 and S3.

Real-time quantitative RT-PCR

RNA was extracted from dissected floral organs and floral buds (8–12 mm) by use of the RNeasy Plant Mini Kit (Qiagen) and treated with RNase-free DNase (Invitrogen) to remove residual DNA. RNA was used as a template for cDNA synthesis with reverse transcriptase and the SuperScript II kit (Invitrogen). For quantitative PCR, the cDNA template was mixed with 2X SYBR Green PCR master mix in an ABI Prism 7000 sequence detection system (Applied Biosystems). The primers used for quantification are given in Supplementary Table S1. Each pair of primers for the TFs *PeMADS1*, *PeMADS6*, and *PebHLH* was developed from specific regions of their nucleotide sequences for real time RT-PCR. For gene quantification, the first blooming flower was collected from three silenced plants that showed VIGS phenotypes. For the real-time RT-PCR reaction, each sample was analysed in triplicate. Reactions involved incubation at 50 °C for 2 min, then 95 °C for 10 min, and thermal cycling for 40 cycles at 95 °C for 15 s and 60 °C for 1 min. After amplification, melting curve analysis was used to verify amplicon specificity and primer dimer formation. Every amplicon in this study yielded similar single peak melting curves, so only the specific products were amplified. Relative quantification followed the manufacturer's instructions (Applied Biosystems). For controlling the integrity of RNA and normalizing target RNA copy numbers in mock-treated and gene-silenced flowers, the housekeeping gene *PeActin* (*PACT4*, AY134752) was amplified by real-time RT-PCR to generate a standard curve of *Actin* mRNA levels (Chen *et al.*, 2005).

RT-PCR

RNA samples were treated with RQ1 DNase (Promega) to remove remnant DNA. Synthesizing the first-strand cDNA involved use of the Superscript II kit (Invitrogen). Gene-specific primer pairs were designed for *PeMADS1*, *PeMADS6*, *PeMADS7*, *PebHLH*, *PebZIP*, and *PeHB*. The *PeActin* gene of *Phalaenopsis* was used as an internal control (Supplementary Table S1). The PCR protocol was initial denaturation at 94 °C for 3 min, then 30 cycles of amplification at 94 °C for 30 s, 55 °C for 30 s, and 72 °C for 1 min, and 72 °C for 3 min. The amplified products were separated on 1% agarose gel, visualized and photographed.

Scanning electron microscopy

For traditional scanning electron microscopy (SEM), samples were fixed in formalin/acetic acid/alcohol. After being dehydrated in an alcohol/acetone series, samples were critical-point dried, sputter-coated with platinum, and observed under a scanning electron microscope (S-4200, Hitachi, Tokyo, Japan) with an accelerating voltage of 15 kV. Photographs were taken with use of a Verichrome pan film (Kodak, Rochester, NY, USA).

For cryo-SEM, samples were dissected and loaded on stubs, frozen with liquid nitrogen slush, then transferred to a sample preparation chamber at –160 °C. After 5 min, when the temperature rose to –130 °C, the samples were fractured. They were etched for 10 min at –85 °C. After being coated at –130 °C, samples were transferred to the SEM chamber and observed at –160 °C with cryo-SEM (Quanta 200 SEM/Quorum Cryo System PP2000TR, FEI, Hillsboro, OR, USA) at 20 kV (Ku *et al.*, 2008).

Characterization of epidermal cell types

The types of superimposed micro-structuring on cell surfaces can be classified into wax film, epicuticular wax crystals, and cuticular folds (Prüm *et al.*, 2012). The shape of the epidermis can be divided into seven types depending on the outline of the epidermis cells and their ratio of width to height. The aspect ratio (β = width/height) of cell types and their terminology is as follows: convex (β ≥ 3/1), hemispherical (β ≧ 2/1), cupola (β < 3/2), conical (β > 3/2), papilla (β < 3/2 and > 1/2), hair papilla (β < 1/3 and > 1/6), and hair (β < 1/7) (Koch *et al.*, 2008).

Measurement of floral organ morphological changes in PeMADS1-, PeMADS6-, *and double-silenced flowers*

To quantify the phenotypic changes of *PeMADS1*-, *PeMADS6*-, and double-silenced plants in various floral organs of the sequence of flowers in an inflorescence, this work tested five plants of two different cultivars (*Dtps.* I-Hsin Sunrise Cinderella 'OX 1357' and *Dtps.* OX Red Shoe 'OX1407'). The proportion of greenish and discoloured areas in floral organs was calculated by use of ImageJ (http://imagej.en.softonic.com/).

The morphological changes of sepals were graded by estimating the proportion of greenish area on the abaxial surface (Supplementary Fig. S3A1), and of petals by estimating the proportion of greenish and discoloured areas on the adaxial surface (Supplementary Fig. S3B1). Lip morphological changes were characterized as three different types and were graded by calculating: (1) the proportion of greenish areas on the abaxial surface of the midlobe and lateral lobes (Supplementary Fig. S3C1); (2) the proportion of flowers that did not develop lateral lobes but contained cirrus (Supplementary Fig. S3C2); and (3) the proportion of flowers that did not develop cirrus and lateral lobes (Supplementary Fig. S3C3). Column morphological changes were characterized as three types and were graded by calculating: (1) the percentage change in length of the column (Supplementary Fig. S3D1); (2) the proportion of flowers showing an abnormal stigmatic cavity (Supplementary Fig. S3D2); and (3) the proportion of flowers showing an abnormal stigmatic cavity and an extra petal-like organ (Supplementary Fig. S3D3).

Results

High-throughput silencing of 126 Phalaenopsis *ESTs*

To identify genes involved in orchid flower morphogenesis, 5593 ESTs had been previously obtained from *P. equestris* flower buds; 152 were predicted as putative TF-related genes (Tsai *et al.*, 2006). This work investigated by high-throughput VIGS whether these TFs play important roles in flower morphogenesis.

Nucleotide sequences from 500 to 3300 bp for the 152 floral TF ESTs were cloned into the CymMV-Gateway vector. The cloning efficiency for inserts <1500 bp was 100% and decreased with inserts >1500 bp; the cloning efficiency was 0 for inserts >3000 bp (Supplementary Fig. S1). Of the 152 TF ESTs studied, 126 were classified into 9 TF families and accounted for 56% of the TF ESTs. The silencing of *PeMADS1*, *PeMADS7*, *PebHLH*, *PeHB*, and *PeZIP* affected flower morphological features and thus flower development (Figs. 1–3 and Supplementary Fig. S4).

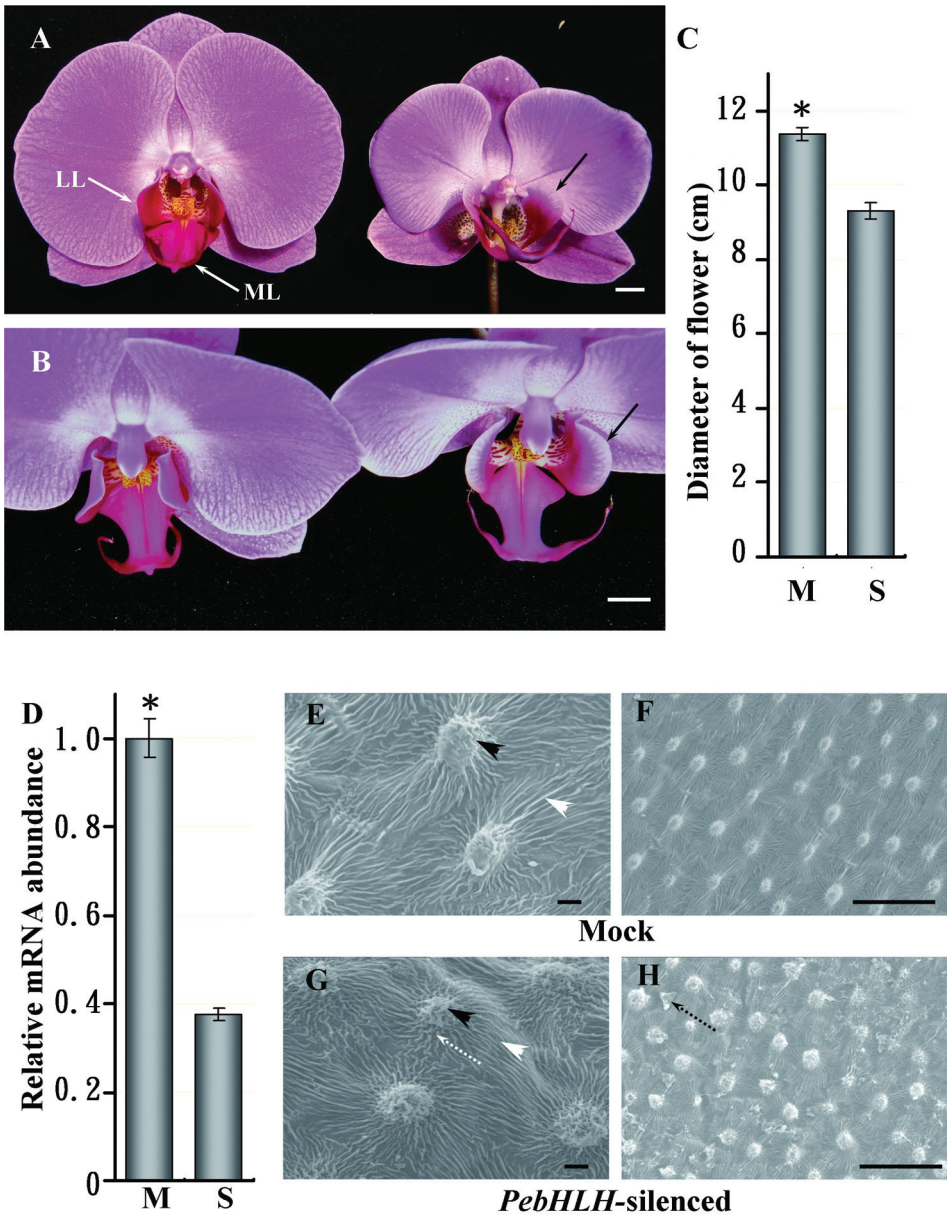

Fig. 1. VIGS phenotypes of *PebHLH*-silenced flowers. (A) Front view of mock-treated (left) and *PebHLH*-silenced flowers (right) in *Doritaenopsis* I-Shin Sunrise Cinderella 'OX1357'; solid white arrows indicate the lateral lobe (LL) and midlobe (ML); solid black arrows indicate the lateral lobes of the lip bowed outward. (B) Top-down view of the lateral lobes of the mock-treated (left) and *PebHLH*-silenced flowers (right); solid black arrows indicate the lateral lobes of the lip bowed outward; white bars, 1 cm. (C) Diameter of flowers in mock-treated and *PebHLH*-silenced plants; a total of four flowers (the 3rd flower at blooming stage) from four plants were examined for each treatment; data are mean ± SD (n = 4); significance was accepted (one-tailed t-test) if $P < 0.01$ (*). (D) Relative level of *PebHLH* in mock-treated and *PebHLH*-silenced flowers. mRNA was extracted from the 3rd floral bud at 15 d post inoculation; data are mean ± SD (n = 4); significance was accepted (one-tailed t-test) if $P < 0.01$ (*). (E–H) SEM of the adaxial surface cells of lateral lobes in lips from mock-treated (E and F) and *PebHLH*-silenced flowers (G and H) at the flower-blooming stage; black arrowheads indicate node-like cuticular folds in the central fields of cells; white arrowheads indicate parallel cuticular folds in the anticline fields of cells; dotted black arrows indicate irregular cuticular folds in the central fields of cells; dotted black arrows indicate epicuticular wax crystals in the anticline field. Bars, 30 μm (this figure is available in colour at *JXB* online).

Silencing PeMADS7, PeHB, *and* PebZIP *resulted in floral abortion*

Silencing *PeMADS7*, *PeHB*, or *PebZIP* caused abortion of the first three floral buds from the bottom of the raceme inflorescence within 2 weeks after agro-infiltration. These aborted flower buds had fully formed sepals, petals, lips, and columns, and their morphological features were unaffected (data not shown). When their expression was restored as the effect of VIGS gradually decreased, the 4th and subsequent floral buds could bloom normally (Supplementary Table S2). The expression of these three genes was detected in the various stages

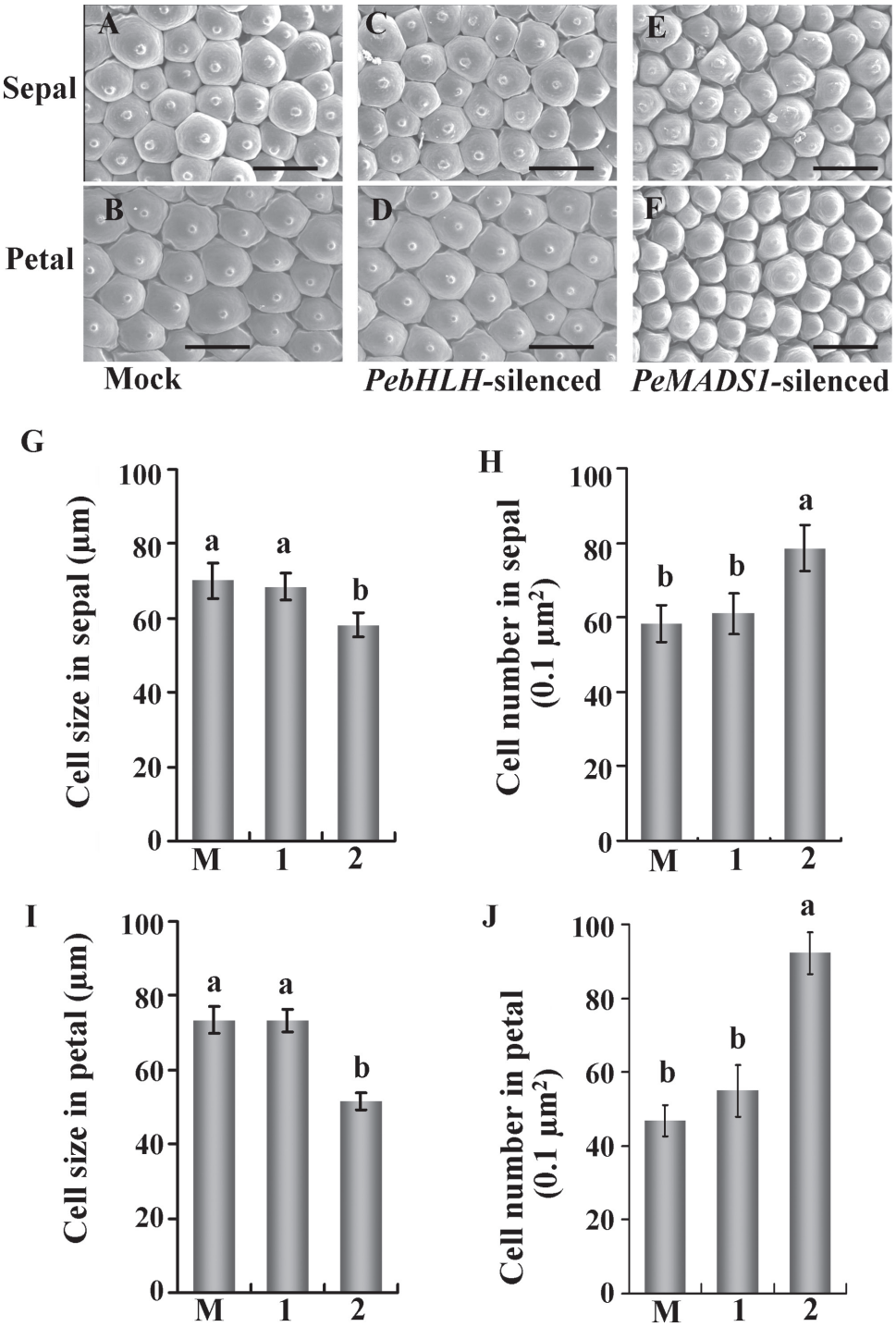

Fig. 2. Silencing of *PebHLH* and *PeMADS1* affects cell size and number in the floral organ. (A–F) SEM of the sepal and petal adaxial surface cells at the flower-blooming stage in mock-treated (A, B), *PebHLH*-silenced (C, D), and *PeMADS1*-silenced flowers (E, F). (G–J) Cell size and cell number in the distal adaxial surface of sepals (G, I) and petals (H, J) in mock-treated (M), *PebHLH*-silenced (1), and *PeMADS1*-silenced flowers (2); data are mean ± SD (n = 6); the same letters above the bars indicate that there is no statistical difference by Duncan's multiple range test ($P < 0.05$) Bar, 30 μm. Materials were *Dtps.* I-Hsin Sunrise Cinderella 'OX 1357'.

of visible floral buds (Supplementary Fig. S2C). Therefore, knockdown of *PeMADS7*, *PeHB*, or *PebZIP* expression allowed the flower to develop normally initially but affected further flower development and growth.

This work performed a BLAST search of the nucleotide sequences of *PeMADS7*, *PeHB*, and *PebZIP* in OrchidBase 2.0 and found no sequences with high similarity to *PeMADS7* or *PebZIP*. Four nucleotide sequences showed high similarity to *PeHB*, with three having more than 21 nt that were 100% homologous to each other (Supplementary Fig. S5). Therefore, the VIGS effects could have resulted from the silencing of *PeHB* and three other *HB* family genes rather than gene-specific effects.

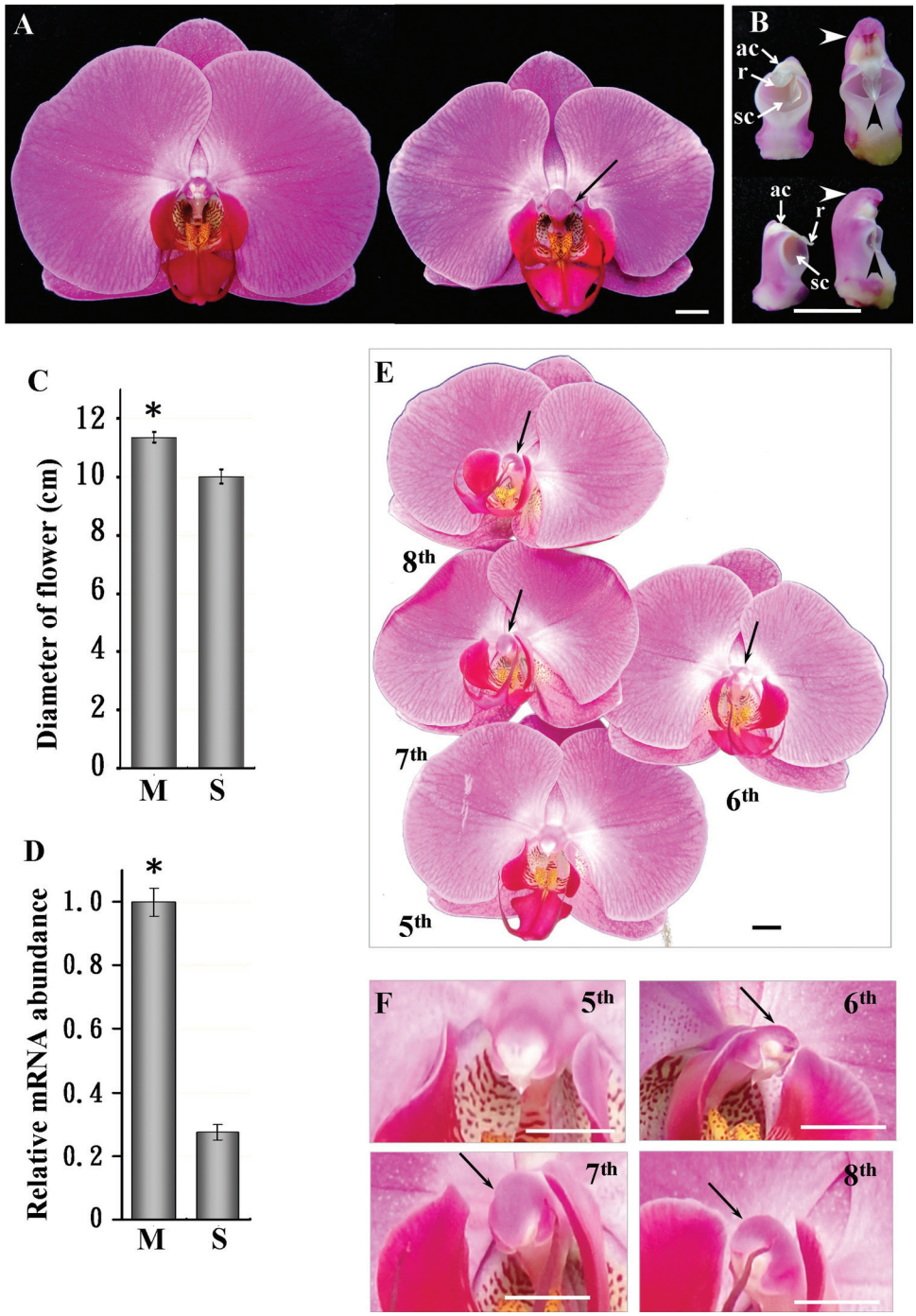

Fig. 3. VIGS phenotypes of *PeMADS1*-silenced flowers. (A) Front view of mock-treated (left) and *PeMADS1*-silenced (right) flowers; solid black arrow indicates a longer and wider column. (B) Front and back view of columns in mock-treated (left) and *PeMADS1*-silenced flowers (right); solid white arrows indicate the anther cap (ac), rostellum (r), and stigmatic cavity (sc); white arrowheads indicate that the opposite site of stigmatic cavity in the column became longer and curved; black arrowheads indicate that the rostellum became longer. (C) Diameter of flowers in mock-treated (M) and *PeMADS1*-silenced plants (S); a total of six flowers (the 7th flower at blooming stage) from six plants were examined for each treatment; data are mean ± SD (n = 6); significance was accepted (one-tailed t-test) if $P < 0.01$ (*). (D) Relative mRNA level of *PeMADS1* in M and S flowers; mRNA was extracted from the 7th floral bud on 35 d post inoculation; data are mean ± SD (n = 6); significance was accepted (one-tailed t-test) if $P < 0.01$ (*). (E) The 5th to 8th blooming flowers in a *PeMADS1*-silenced inflorescence and (F) columns of the 5th to 8th flowers; solid black arrows indicate that the column became longer and wider. Bars, 1 cm.

VIGS of PebHLH *affected regulation of floral size and cell arrangement*

Flower size was significantly reduced in *PebHLH*-silenced plants (Fig. 1A and Supplementary Fig. S4A). In addition, the lateral lobes of the lip bowed outward and their angle to the column was larger than in mock-treated plants (Fig. 1A and B). Adaxial epidermal cells of lip lateral lobes in *PebHLH*-silenced plants lost their organized arrangement (Fig. 1F and H), but they retained their convex shape (Fig. 1E and G) and accumulated epicuticular wax crystals in the anticline field of cells (Fig. 1F and H). The diameter was smaller, by 17.9%, for *PebHLH*-silenced than mock-treated flowers (Fig. 1A and C). The relative mRNA level of *PebHLH* in the floral organs was significantly reduced, by 62.3 ± 4.7% (Fig. 1D).

To analyse whether the reduced floral organ size in the *PebHLH*-silenced flowers was due to a defect in cell expansion, this work examined cell size and cell number per 0.1 μm^2 surface area of the adaxial epidermis of sepals and petals by SEM. The epidermal cell shape in *PebHLH*-silenced flowers remained papilla shaped, as for mock-treated flowers (Fig. 2A–D). In addition, the adaxial epidermal cell size and cell number per 0.1 μm^2 surface area was similar for *PebHLH*-silenced and mock-treated sepals and petals (Fig. 2G–J). Thus, silencing *PebHLH* did not affect cell morphological features, cell size, or cell number per unit area. The reduced flower size could be due to premature termination of proliferation or reduction of final cell number in sepals and petals.

The phylogeny of *PebHLH* was determined with all existing 158 (26 subfamilies) and 173 basic helix–loop–helix (*bHLH*) (27 subfamilies) gene sequences from *Arabidopsis* and rice, respectively (Pires and Dolan, 2010). *PebHLH* was in the same clade as *AtbHLH149* set apart from the 27 subfamilies, and thus could be classified as an 'orphan' (Supplementary Fig. S6). *PebHLH* was expressed in roots, leaves, and all developmental stages of floral organs in *Phalaenoopsis* (Supplementary Fig. S2C and F).

VIGS of PeMADS1 resulted in a homeotic conversion in column and reduced cell size

PeMADS1 expression was detected in the floral meristem and all developmental stages of floral buds (Supplementary Fig. S2C). In *PeMADS1*-silenced flowers, the 6th to 8th flowers in a raceme inflorescence had an enlarged and wide column, with the most severe phenotypic changes on the 7th flower (Fig. 3A, B and E, F). The diameters of flowers were reduced by 11.8% in *PeMADS1*-silenced plants (Fig. 3A and C), and the mRNA level of *PeMADS1* was significantly decreased by 72.4% in silenced plants (Fig. 3D).

On SEM, adaxial epidermal cells in the sepal and petal in *PeMADS1*-silenced flowers were 17% and 30% smaller, respectively, than those of mock-treated flowers (Fig. 2G and I). The reduced cell size was accompanied by increased cell number in the same surface area in *PeMADS1*-silenced flowers (Fig. 2H and J). Therefore, small floral organ size in *PeMADS1*-silenced plants was primarily caused by reduced cell expansion.

The epidermal cell shape of sepals and petals was the same in *PeMADS1*-silenced and mock-treated flowers (Fig. 2E and F). However, the rostellum of the column was longer in *PeMADS1*-silenced than mock-treated flowers. The anther cap, which covers the end of the column, was located on the same side as the stigmatic cavity in *PeMADS1*-silenced flowers (Fig. 3B).

In addition, the epidermal cells of *PeMADS1*-silenced columns (Fig. 4N) were changed and similar to that of the adaxial surface of mock-treated petals (Fig. 4C). Epidermal cells of mock-treated columns showed cuticular folds in the central field (Fig. 4G). In contrast, *PeMADS1*-silenced columns showed a protuberance on the top of cells and no cuticular folds in the central field (Fig. 4N). Thus, the column of *PeMADS1*-silenced flowers exhibited a partial homeotic transformation to petal-like.

Co-silencing B- and C-class MADS-box genes caused a petal-like lip and column

To investigate the additive effect of B- and C-class MADS-box gene expression on orchid floral morphogenesis, *PeMADS1* and *PeMADS6* fragments constructed in separate vectors were co-infiltrated. These two genes were expressed in various stages of visible floral buds (Supplementary Fig. S2C). Previously, silencing *PeMADS6* alone caused leaf-like sepals and a petal-like lip (Hsieh *et al.*, 2013). In this study, silencing *PeMADS1* alone caused a petal-like column. For double silencing, *Phalaenopsis* plants were inoculated with a mixture of *Agrobacterium* cultures containing pCAMBIA-CymMV-*PeMADS1* and -*PeMADS6* at a 1:1 ratio. In the positive control, the greenish and discoloured phenotype appeared in the sepals, petals, and lip of the first eight blooming flowers of *PeMADS6*-silenced plants, with the first three not able to bloom normally (Supplementary Fig. S7E). In contrast, with double-silencing *PeMADS1* and *PeMADS6*, a similar effect was detected only from the 1st to the 6th blooming flowers; the phenotypic changes were most severe in the first flower and weakened with each consecutive flower (Supplementary Fig. S7F). In the first blooming flower, the margins of sepals and petals were curly and discoloured (Fig. 5E–H), and the lip was greenish and discoloured (Fig. 5G) as compared with mock-treated flowers (Fig. 5A–D).

The combined silencing phenotype of lip and columns was detected in the 7th blooming flowers in the same inflorescence approximately 58 d after agro-infiltration (Fig. 5I–L). The lip lacked cirrus and the lateral lobes fused with the mid-lobe into a petal-like lip (Fig. 5K). The column did not develop a circle-shaped stigmatic cavity, and in some cases, extra anther cap-like and rostellum-like structures appeared at the end of the column (Fig. 5L). Therefore, both *PeMADS1* and *PeMADS6* play important roles to ensure the normal development of lip and column. Similar phenomena were observed with the double silencing of *PeMASD1* and *PeMADS6* in three different cultivars, *Dtps.* I-Hsin Sunrise Cinderella 'OX1357', *Dtps.* OX Red Shoe 'OX1407', and *P.* Sogo Yukidian 'V3' (Supplementary Fig. S7 and S8 and Supplementary Table S3).

Epidermal cellular changes with co-silencing B- and C-class MADS-box genes

In mock-treated flowers, the sepal adaxial epidermal cells had a polygonal and papilla shape with a protuberance on the top of cells (Figs. 4A and 6A), and the abaxial ones had an irregular and convex shape (Figs. 4B and 6B). The shapes of adaxial and abaxial epidermal cells of the petal were similar to those of the sepal (Figs. 4C, D and 6C, D). The lip adaxial and abaxial epidermal cells contained irregular cuticular folds in the central fields and parallel cuticular folds in the anticline fields (Figs. 4E, F and 6E, F). However, the lip adaxial epidermal cells had a polygonal and convex shape (Figs. 4E and 6E), and the abaxial ones had an elongated polygonal and convex shape (Figs. 4F and 6F). The column epidermal cells had a polygonal and conical shape with irregular cuticular folds in the central fields and parallel cuticular folds in the anticline fields (Figs. 4G and 6G).

PeMADS1-silenced flowers showed significant phenotypic changes in the lip and column epidermal cells (Figs. 4L–N and 6L–N). In the adaxial epidermal cells of the lip, the parallel epicuticular folds were replaced with irregular ones in the anticline fields (Figs. 4L and 6L). The irregular epicuticular folds in the abaxial epidermal cells of the lip were replaced with parallel ones in the central fields (Figs. 4M and 6M). A protuberance appeared on the top of column epidermal cells (Figs. 4N and 6N).

PeMADS6-silenced flowers showed significant phenotypic changes in the sepal, petal and lip epidermal cells (Figs. 4O–U and 6O–U). The adaxial and abaxial epidermal cells of sepals in greenish areas (Supplementary Fig. S7E) were convex shaped, with epicuticular wax crystals (Figs. 4O, P and 6O, P). The adaxial epidermal cells of petals in greenish areas had papilla and hair papilla shapes (Figs. 4Q and 6Q) and the surface of epidermis was not flat (Supplementary Fig. S9K). The adaxial and abaxial epidermal cells of the lip in greenish areas lost the cuticular folds covering the cells (Figs. 4S, T and 6S, T). In addition, the adaxial cells had a conical shape (Fig. 4S and 6S) and an irregular arrangement in epidermis (Supplementary Fig. S9S).

The first blooming flowers of double-silenced plants showed significant phenotypic changes in the sepal (Supplementary Fig. S10Q, R and X, Y) and lip (Supplementary Fig. S10U, V and AB, AC). The adaxial and abaxial epidermal cells of sepals in greenish areas were all irregular and convex shaped, with cuticular wax crystals (Supplementary Fig. S10Q, R and X, Y), which was similar to those of leaves (Supplementary Fig. S10H and I). The adaxial epidermal cells of the lips with greenish areas were irregular and cupola shaped, with a protuberance on the top of cells (Supplementary Fig. S10U and AB).

Petal-like lip and column epidermal cells in the 7th blooming flowers of double-silenced plants showed significant phenotypic changes (Figs. 4Z–AB and 6Z–AB). The adaxial epidermal cells of the petal-like lip had an irregular and hemispherical shape with a protuberance on the top of cells and thin, dense cuticular folds (Figs. 4Z and 6Z), while the abaxial ones lost irregular cuticular folds in the central fields (Figs. 4AA and 6AA). The column epidermal cells had an elongated polygonal form (Fig. 4AB) and different shapes including convex, hemispherical, cupola, conical, and papilla (Fig. 6AB and S9AB).

Thus, *PeMADS6*-silenced plants showed a homeotic transformation in the epidermal cells in the greenish areas of the lip. The epidermal cells of *PeMADS1*-silenced lips showed slight changes in structure. Double-silenced plants went through a homeotic transformation from a lip to a petal-like lip in greenish areas. However, their epidermal cells showed only slight changes in shape and structure.

Double-silenced flowers showed more significant changes in the column and lip than single-silenced flowers

The severity of floral organ morphological changes was quantified for sequences of flowers from *PeMADS1*-, *PeMADS6*-, and double-silenced plants (Supplementary Fig. S3A–D). Greenish areas of the sepal, petal and lip appeared only in *PeMADS6*- and double-silenced plants but not *PeMADS1*-silenced plants (Fig. 7A–C). Approximately eight flowers of each inflorescence showed the VIGS phenotype in *PeMADS6*- and double-silenced plants, beginning with the bottom of the raceme (Fig. 7A–E and G–H). However, three *PeMADS1*-silenced flowers showed morphological changes in the column from the 6th to the 8th flowers (Fig. 7F). The most severe morphological change occurred in the 7th flower, followed by the 8th and then 6th flower (Fig. 7F). The VIGS phenotype lasted longer for *PeMADS6*- than *PeMADS1*-silenced plants (Fig. 7A–C and F), so the period of floral development affected by loss of function lasted longer for *PeMADS6*- than *PeMADS1*-silenced plants.

In *PeMADS6*-silenced plants, the greenish areas in the sepal were gradually reduced from 73.9% in the 1st flower to zero in the 9th flower (Fig. 7A), while the greenish and discoloured areas in the petal and lip were reduced from 32.3% and 25.8% to zero, respectively (Fig. 7B, C). In double-silenced plants, the greenish areas of the sepal were gradually reduced from 7.4% in the 1st flower to zero in the 9th flower (Fig. 7A), while the greenish and discoloured areas in the petal and lip were reduced from 10.7% and 13.1% to zero, respectively (Fig. 7B, C). Thus, VIGS phenotypic changes were less in flowers of double-silenced than *PeMADS6*-silenced plants.

In addition, in 30% of the double-silenced plants, the 7th flower did not develop lateral lobes (Fig. 7D), 20% did not develop cirrus and lateral lobes on the lip (Fig. 7E), 30% developed an abnormal stigmatic cavity (Fig. 7G), and 20% developed an abnormal stigmatic cavity as well as an extra petal-like organ on the column (Fig. 7H). Thus, both genes were silenced simultaneously within both the 7th and 8th blooming flowers.

The silencing effect of *PeMADS6* was assessed by comparing the mRNA levels of odd-numbered mock-treated and *PeMADS1*-, *PeMADS6*-, and double-silenced flowers (Fig. 8A-D). The *PeMADS6* mRNA levels were lower in *PeMADS6*- and double-silenced sepals, petals, lips, and columns from the 1st to the 5th blooming flowers than in mock-treated and *PeMADS1*-silenced parts (Fig. 8A–D). Interestingly, the *PeMADS6* mRNA levels were sharply reduced to 4.7% and 13.9% in the 7th blooming flower of

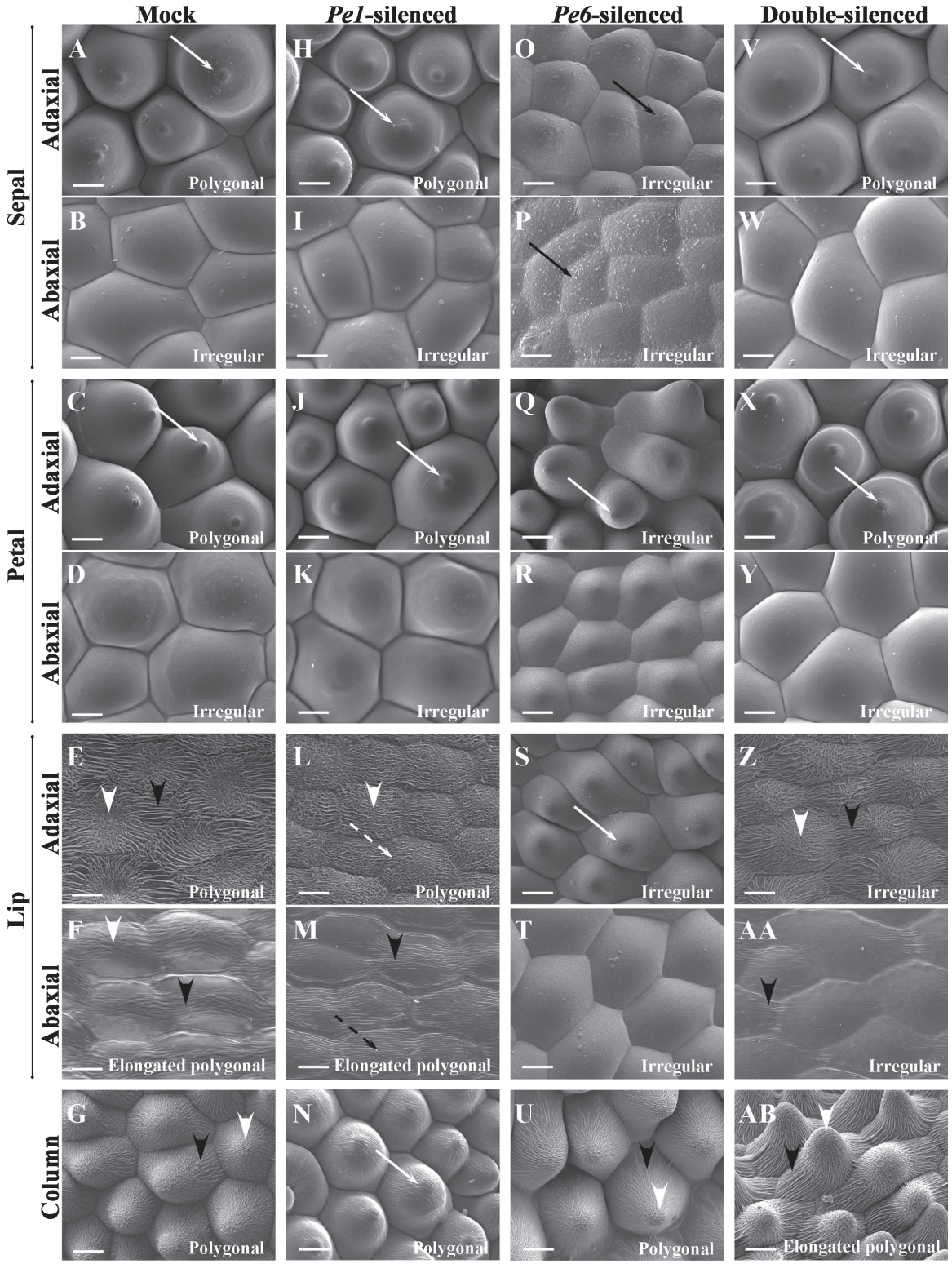

Fig. 4. Cyro-SEM micrographs of top views of epidermal cells of floral organs of the 7th blooming flowers of mock-treated (A–G), *PeMADS1*-silenced (H–N), *PeMADS6*-silenced (O–U), and double-silenced floral organs (V–AB). (A, H, O, V) Sepal adaxial epidermal cells had polygonal, polygonal, irregular, and polygonal forms. (B, I, P, W) Sepal abaxial epidermal cells all had irregular forms. (C, J, Q, X) Petal adaxial epidermal cells had polygonal, polygonal, irregular, and polygonal forms. (D, K, R, Y) Petal abaxial epidermal cells all had irregular forms. (E, L, S, Z) Lip adaxial epidermal cells had polygonal, polygonal, irregular, and irregular forms. (F, M, T, AA) Lip abaxial epidermal cells had elongated polygonal, elongated polygonal, irregular, and irregular forms. (G, N, U, AB) Column epidermal cells had polygonal, polygonal, polygonal, and elongated polygonal forms. Solid white arrows indicate a protuberance on the top of the cell; solid black arrow indicates epicuticular wax crystals; white arrowheads indicate irregular cuticular folds in the central field; black arrowheads indicate parallel cuticular folds in the central field; dashed white arrows indicate irregular cuticular folds in the anticline field; dashed black arrows indicate parallel cuticular folds in the central field. Bars, 25 μm. Materials were *Dtps.* OX Red Shoe 'OX1407'.

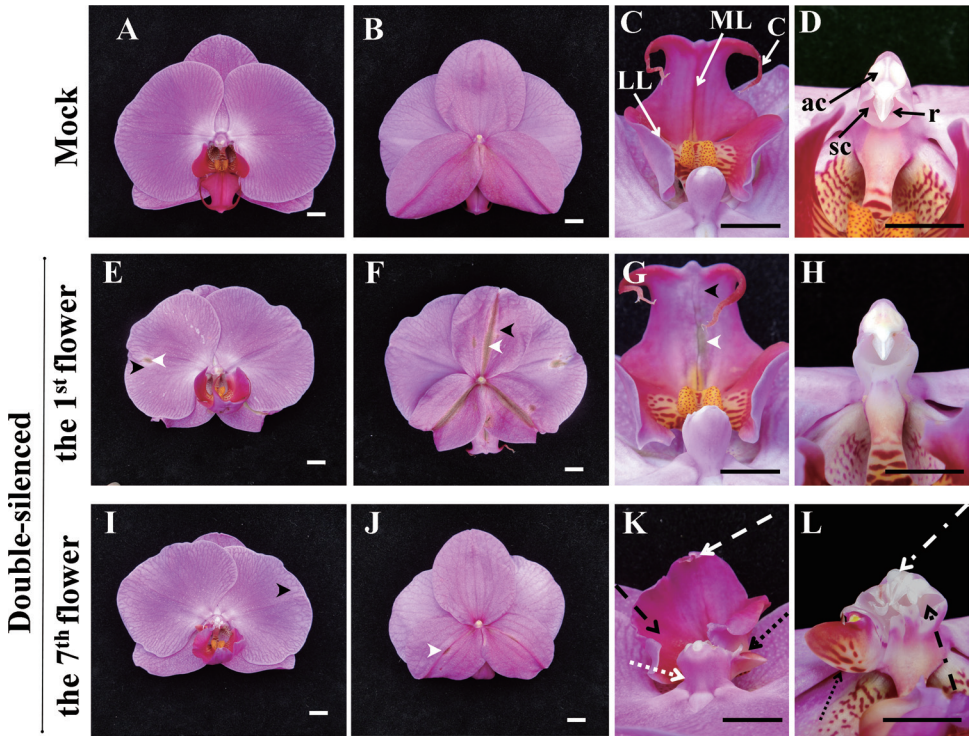

Fig. 5. Concurrent silencing of both *PeMADS1* and *PeMADS6* with a pCymMV-Gateway vector. (A–D) Mock-treated plants: top view (A), back view (B) of the flower and front view of lip (C) and column (D); solid white arrows indicate the lateral lobe (LL) and midlobe (ML); solid black arrows indicate the anther cap (ac), rostellum (r), stigmatic cavity (sc), and cirrus (C). (E–H) 1st blooming flower of double-silenced plants: top view (E), back view (F), and front view of lip (G) and column (H); black arrowheads indicate discoloured characteristics of sepals, petals, and lips; white arrowheads indicate dark green colouration (including leaf-like characteristics) of sepals, petals, and lips. (I–L) 7th blooming flower of double-silenced plants: top view (I), back view (J), and front view of lip (K) and column (L); dashed white arrow indicates that no cirrus developed in the tip of the midlobe; dashed black arrow indicates that the lateral lobes and midlobe were fused into a petal-like lip; dotted white arrow indicates that the base of the column became wider; dotted black arrows indicate that the side of the column developed an extra petal-like organ; dash-dotted white arrow indicates that the anther cap became wider and the appearance of more than one rostellum-like organ; dash-dotted black arrow indicates that the stigmatic cavity did not develop normally. White bars and black bars, 1 cm.

double-silenced lip and column, respectively. As expected for very little phenotypic changes, the *PeMADS6* mRNA levels increased again and reached just over 60% in the 9th blooming flower (Fig. 8C, D).

Real-time RT-PCR analysis showed that the levels of *PeMADS1* expression in the sepal, petal, and lip were generally at least 2000–5000-fold lower than found in the column in mock treated flowers (data not shown). The *PeMADS1* mRNA levels were significantly lower in *PeMADS1*-, *PeMADS6*-, and double-silenced columns from the 1st to the 5th blooming flowers in mock-treated columns (Fig. 9D). Interestingly, the *PeMADS1* mRNA levels of *PeMADS1*-silenced and double-silenced flowers were further reduced to 17.7% and 6.2% in the 7th blooming flower (Fig. 9D). These results suggests that the *PeMADS1* mRNA levels were mainly affected in the 7th blooming flowers of double-silenced plants, but the *PeMADS6* mRNA levels were all affected from the 1st to the 7th blooming flowers.

Discussion

Among angiosperms, orchids are unique in their floral patterning, particularly in the lip and column structures. To uncover the role of specific TFs in floral development, this work used high-throughput VIGS with the CymMV-Gateway vector and shows the genetic interactions between B- and C-class MADS-box genes, namely *PeMADS6* and *PeMADS1*, in determining proper patterning of floral organs by transiently downregulating both genes in a non-model plant, the orchid.

In high-throughput VIGS for floral genomics, *PeMADS1*, a C-class *AGAMOUS*-like MADS-box gene (Tsai *et al.*, 2008), was identified as being involved in the normal development of the column and affecting floral size. Previous studies showed that loss of function of C-class MADS-box genes caused homeotic transformations of reproductive organs into perianth organs in petunia (Kapoor *et al.*, 2002) and tomato (Pnueli *et al.*, 1994) and reduced floral size in *Antirrhinum* (Bradley *et al.*, 1993), *Arabidopsis* (Yanofsky *et al.*, 1990), wheat (Aida *et al.*, 2003), and Chinese narcissus (Deng *et al.*, 2011). In *Phalaenopsis*, *PeMADS1* may also regulate floral organ size primarily by affecting cell size.

In *PeMADS1*/*PeMADS6*-silenced plants, this study present a schema of period of development that is most sensitive to loss of function with agro-infiltration in an inflorescence containing eight internodes and one visible floral bud (Supplementary Fig.

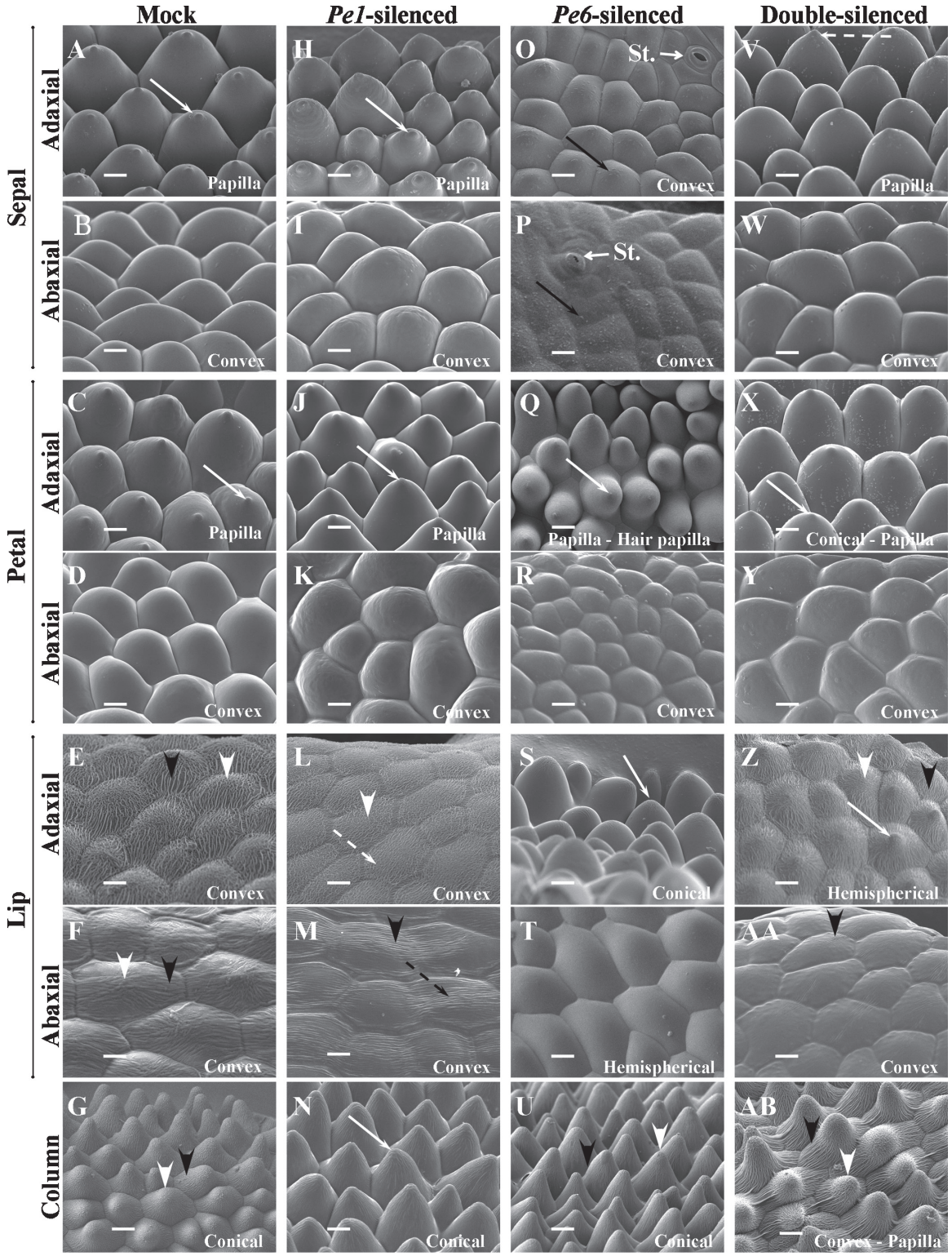

Fig. 6. Cyro-SEM micrograph of side views of epidermal cells of floral organs of the 7th blooming flowers of mock-treated (A–G), *PeMADS1*-silenced (H–N), *PeMADS6*-silenced (O–U), and double-silenced floral organs (V–AB). (A, H, O, V) Sepal adaxial epidermal cells had papilla, papilla, convex, and papilla shapes. (B, I, P, W) Sepal abaxial epidermal cells all had convex shape; St., stomata. (C, J, Q, X) Petal adaxial epidermal cells had papilla, papilla, papilla/hair papilla, and conical/papilla shapes. (D, K, R, Y) Petal abaxial epidermal cells all had convex shapes. (E, L, S, Z) Lip adaxial epidermal cells had convex, convex, conical, and hemispherical shapes. (F, M, T, AA) Lip abaxial epidermal cells had convex, convex, hemispherical, and convex shapes. (G, N, U, AB) Column epidermal cells had conical, conical, conical, and different shapes (including convex, hemispherical cupola, conical, and papilla). Solid white arrows indicate a protuberance on the top of the cell; solid black arrow indicates epicuticular wax crystals; white arrowheads indicate irregular cuticular folds in the central field; black arrowheads indicate parallel cuticular folds in the central field; dashed white arrows indicate irregular cuticular folds in the anticline field; dashed black arrows indicate parallel cuticular folds in the central field. Bars, 25 μm. Materials were *Dtps.* OX Red Shoe 'OX1407'.

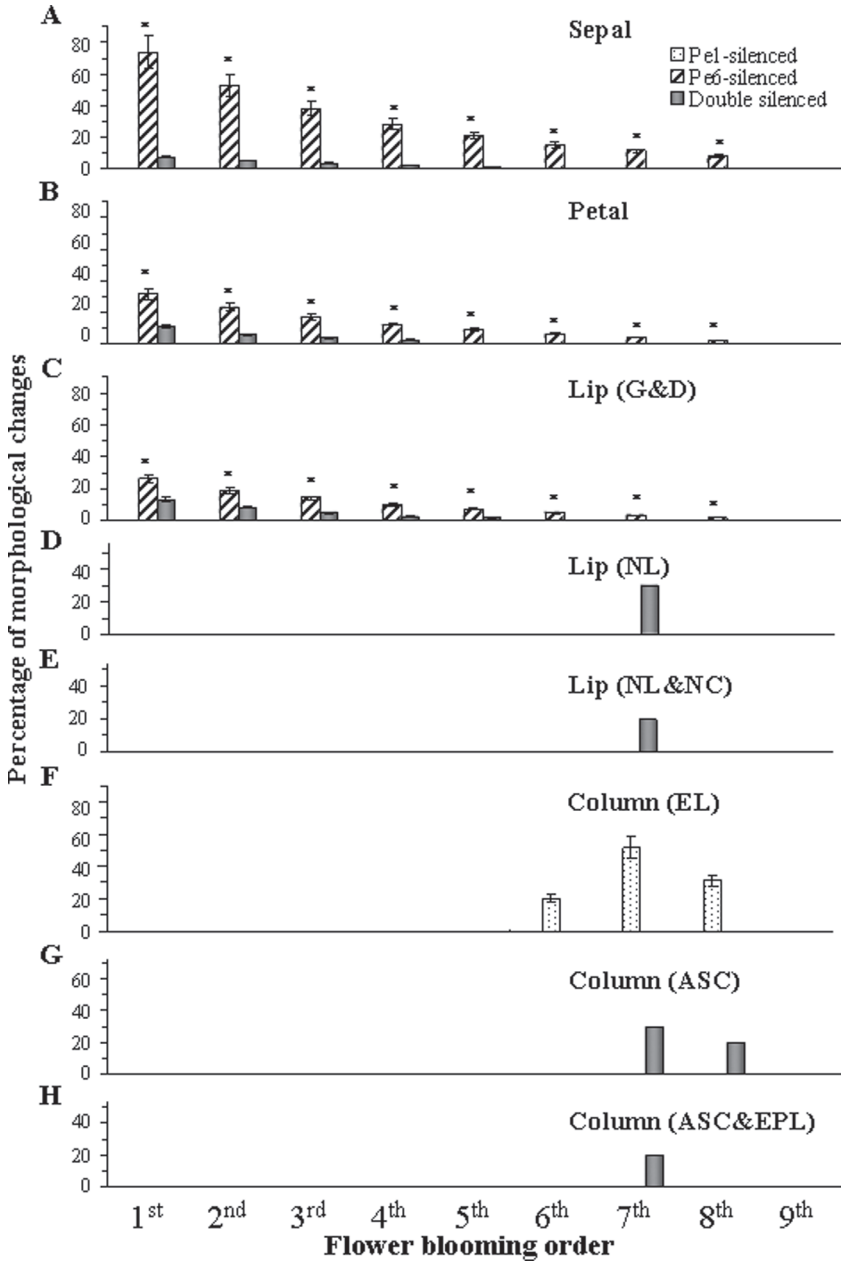

Fig. 7. Severity of floral organ morphological changes in ordered blooming flowers in *PeMADS6*- (dotted bars), *PeMADS1*- (slash bars), and double-silenced plants (black bars). (A) Sepal morphological changes graded by estimating the percentage of greenish area on the abaxial surface. (B) Petal morphological changes graded by estimating the percentage of greenish and discoloured areas on the adaxial surface. (C–E) Lip morphological changes graded by estimating the percentage of greenish and discoloured areas on the abaxial surface of the midlobe and lateral lobes (C, G&D, greenish and discoloured), calculating the percentage of flowers that did not develop lateral lobes (D, NL, no lateral lobes), and he percentage of flowers that did not develop cirrus as well as the lateral lobes (E, NL&NC, no lateral lobes and no cirrus). (F–H) Column morphological changes were graded by calculating the percentage change in the length of the column (F, EL, elongated length of column; the formula is (length of VIGS column – length of mock column)/(length of mock column) ×100, calculating the percentage of flowers that developed an abnormal stigmatic cavity (G, ASC), and the percentage of flowers that developed an abnormal stigmatic cavity as well as an extra petal-like organ (H, ASC&EPL). Significance was accepted (one-tailed t-test) if $P < 0.01$ (*).

S11). In observing the anatomy of a *Phalaenopsis* inflorescence tip, the development of the inflorescence containing one visible floral bud can be divided into four major stages: stage 1, the formation of floral primordia; stage 2, the formation of early floral organ primordia with sepals, petals, lip, and column; stage 3, the formation of late floral organ primordia with pollina and callus developing on the column and the lip, respectively; and stage 4, the development and enlargement of floral buds (Pan *et al.*, 2011). The floral buds in an inflorescence could be sensitive to loss of function from stage 2 to 4 with *PeMADS6* silencing and sensitive to loss of function from stage 2 to 3 with *PeMADS1* silencing (Supplementary Fig. S11).

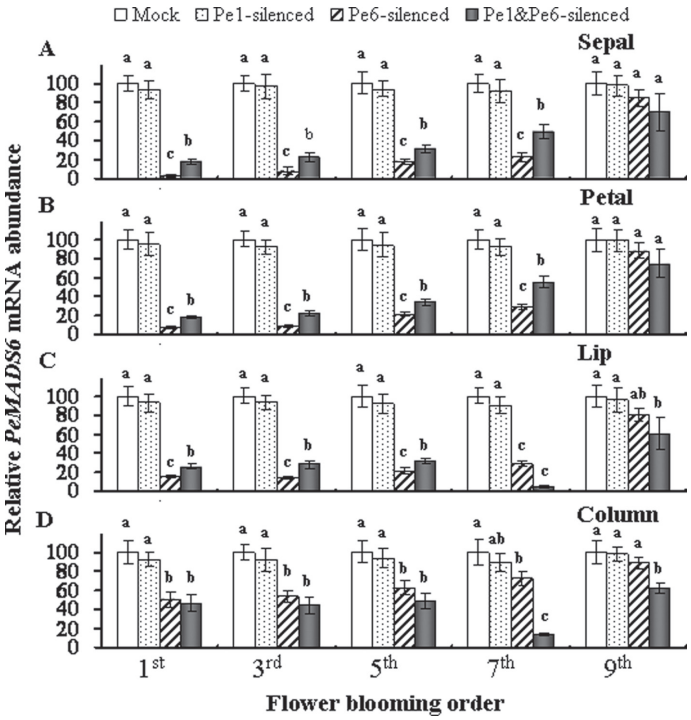

Fig. 8. Expression of *PeMADS6* in *PeMADS1*-, *PeMADS6*-, and double-silenced plants according to flower blooming order (1st, 3rd, 5th, 7th, and 9th) in inflorescences of mock-treated plants (Mock) and *PeMADS1*-, *PeMADS6*-, and double-silenced plants (Pe1-silenced, Pe6-silenced, and Pe1&Pe6-silenced) in the (A) sepal, (B) petal, (C) lip, and (D) column. mRNA was extracted at flower blooming date in *Dtps.* I-Hsin Sunrise Cinderella 'OX 1357'. Data are mean ± SD from three plants for each experiment (n = 3); the same letters above the bars indicate that there is no statistical difference by Duncan's multiple range test ($P < 0.05$).

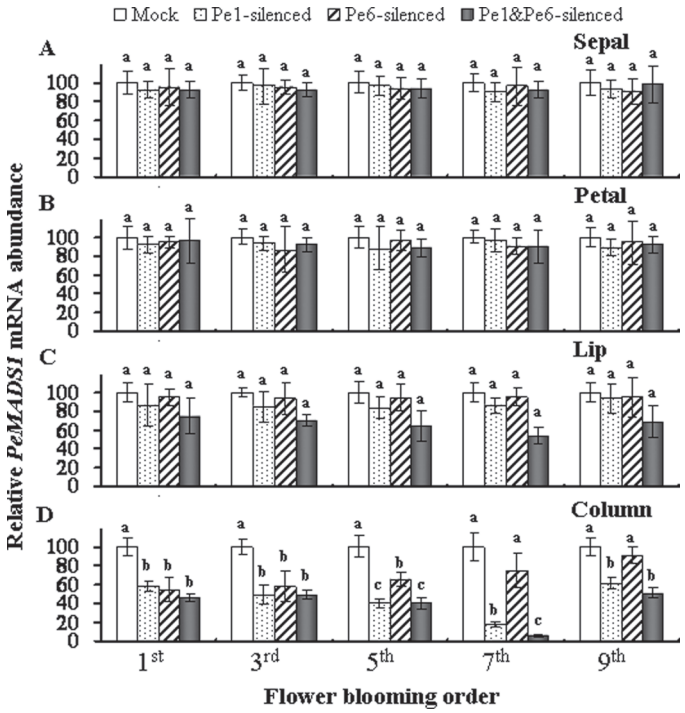

Fig. 9. Expression of *PeMADS1* in *PeMADS1*-, *PeMADS6*-, and double-silenced plants according to flower blooming order (1st, 3rd, 5th, 7th, and 9th) in inflorescences of mock-treated plants (Mock) and *PeMADS1*-, *PeMADS6*-, and double-silenced plants (Pe1-silenced, Pe6-silenced, and Pe1&Pe6-silenced) in the (A) sepal, (B) petal, (C) lip, and (D) column. mRNA was extracted at flower blooming date in *Dtps.* I-Hsin Sunrise Cinderella 'OX 1357'. Data are mean ± SD from three plants for each experiment (n = 3); the same letters above the bars indicate that there is no statistical difference by Duncan's multiple range test ($P < 0.05$).

The flowers of double mutants of B- and C-class genes, such as *pi ag* and *ap3 ag*, consist entirely of sepal-like organs, and their flowers are indeterminate with flowers within flowers in *Arabidopsis* (Bowman *et al.*, 1989). Similarly, in rice flowers, both B- and C-class gene mutants (*spw1-1 osmads3-4* and *spw1-1 osmads58*) show carpelloid structures and glume-like organs but appear to have morphological features similar to that of the marginal region of the wild-type palea (Yun *et al.*, 2013). The current work observed extra petal-like organs at the position of column and petal-like epidermal cells in the lip in *PeMADS6* and *PeMADS1* double-silenced flowers. In addition, the lip was transformed into a petal-like organ. Although the flowers showed partial homeotic conversions of floral organs into petals, they were unlike the *bc* mutants of *Arabidopsis* (*ap3 ag* and the *pi ag*) or rice (*spw1-1 osmads3-4* and *spw1-1 osmads58*), that have indeterminate flowers composed only of sepal-like organs or carpelloid flowers, respectively (Bowman *et al.*, 1991; Coen and Meyerowitz, 1991; Meyerowitz *et al.*, 1991; Yun *et al.*, 2013). *PeMADS6*-silenced plants show petal-like lip and leaf-like sepal epidermal cells (Hsieh *et al.*, 2013). In *PeMADS1*-silenced plants, the column became longer and wider. However, *PeMADS6* and *PeMADS1* double-silenced flowers showed severe phenotypic changes in the column as compared with *PeMADS1*-silenced flowers because *PeMADS6* and *PeMADS1* are both expressed only in the column (Tsai *et al.*, 2005; Song *et al.*, 2006). In addition, phenotypic changes were more severe in double-silenced than *PeMADS6*-silenced lips, which further suggests that the interaction of B- and C-class genes may dictate the lip morphogenesis.

The epidermal cell surfaces of sterile whorl organs in *Phalaenopsis* flowers are distinctive (Bercu *et al.*, 2011). The varieties of cell shape and superimposed micro-structuring are important factors that affect how flowers interact with the abiotic environment (influencing light capture and reflectance, evaporation, temperature, and wetness) and the biotic environment (providing visual, tactile, and olfactory cues to pollinating animals) (Whitney *et al.*, 2011). The changes in epidermal features alone can be considered a homeotic transformation in floral morphogenesis (Vandenbussche *et al.*, 2004). In addition, epidermal cell shape is frequently used to determine floral organ identity in floral organs showing a homeotic transformation (Chang *et al.*, 2010). In the *PhGLO1* mutant plants of *Petunia hybrida*, flowers showed a conversion of the typical conical petal epidermal cells into sepal-like epidermal cells with the presence of stomata as well as the development of trichomes, which suggests a shift of the petal toward a

sepal identity in these regions (Vandenbussche *et al.*, 2004). Double *NbGLO1-NbGLO2*-VIGS (B-class MADS gene-silenced) *Nicotiana benthamiana* flowers showed a strong conversion of petals into sepals with the presence of stomata, numerous trichomes as well as puzzle-shaped epidermal cells. The petal-to-sepal transformation was also evident in the abaxial and adaxial epidermal cells of the petal, which were morphologically similar to those of wild-type sepals (Geuten and Irish, 2010). In rice flowers, the shape and the arrangement of epidermal cells of the carpel-like organs of C-class gene mutants (*osmads58-s1*) were almost identical to those of the wild-type carpel wall. Furthermore, the surface morphological aspects of the carpel-like organs differed from those of wild-type palea and lemma (Yamaguchi *et al.*, 2006). In both *spw1-1 osmads3-4* and *spw1-1 osmads58* (B- and C-class gene mutants) flowers, the epidermal cells of both abaxial and adaxial surfaces of glume-like organs showed a smooth morphological aspect and no trichomes, which was similar to cells of the marginal region of wild-type paleas.

In *Phalaenopsis*, the shape of *PeMADS6*-silenced epidermal cells from the greenish or discoloured areas of the lip was almost identical to that of mock-treated petals. In addition, sepal epidermal cells covered by a cuticle film were similar to those of mock-treated leaves. This finding could be due to B-class gene functions possibly acting in primordia to establish identity and also late in development to achieve the proper final morphological features of conical cells in the petal epidermis, which occurs in *Antirrhinum* (Zachgo *et al.* 1995). The conical epidermal cell may be a hallmark for petaloid organs, possibly aiding pollinator orientation on flowers (Kramer and Hodges, 2010; Whitney *et al.*, 2011).

In cotton, an *AGAMOUS* (*AG*)-like gene, *GbAGL2*, specifies the identity of floral organs and potentially plays a key role in fibre development (Liu *et al.*, 2009). In *Phalaenopsis amabilis*, the sepal and petal structures are similar, with papillose cells in the adaxial epidermis and a few stomata in the abaxial surface. Lip epidermal cells appear elliptical in form, not papillose shaped, and are covered by a striate cuticle (Bercu *et al.*, 2011). In double-silenced *Phalaenopsis*, the conical and convex shapes of the lip cells of the 1st blooming flowers were similar to the epidermal cells of mock-treated petals and *PeMADS6*-silenced lips. In the 7th blooming flowers, the abaxial epidermal cells of the petal-like lip lacked cuticular folds in the central fields, and the adaxial ones had fewer and thinner cuticular folds in the anticline fields than in the mock-treated lip. *PeMADS6* and *PeMADS1* genes might specify the identity of floral organs and potentially play a key role in cuticle development.

This study identified *PebHLH* involved in the expression of floral development by high-throughput VIGS. The functions of most *bHLH* genes are conserved during angiosperm evolution (Li *et al.*, 2006). *SPATULA* (*SPT*), a *bHLH* transcription factor, controls the development of the carpel margins in *Arabidopsis* (Heisler *et al.*, 2001). Silencing *bHLH* transcription factors, such as *ANTHOCYANIN1*, *BIGPETAL*, and *SPT*, can cause several changes depending on the plant. In *Arabidopsis*, silencing *BIGPETAL* increased petal size because of increased cell size and number (Szecsi *et al.*, 2006; Varaud *et al.*, 2011). Loss of function of *SPT* increased leaf size and total cell number, but cell size was not affected (Ichihashi *et al.*, 2010). *PebHLH* is in the same clade as *AtbHLH149* (*AIF4*) of *Arabidopsis*. *AIF4* is a *bHLH* DNA-binding superfamily protein, which negatively regulates cell elongation (Wang *et al.*, 2009; Ikeda *et al.*, 2013). *PebHLH*-silenced plants showed curved floral organs, for a change in flower size. Therefore, *PebHLH* might affect total cell number for the whole floral organ and have a wide variety of functions in *Phalaenopsis*.

In conclusion, in a large-scale screening of gene functions related to floral morphogenesis in *Phalaenopsis*, this study found that knocking down the expression of individual TFs, including *PebHLH* and *PeMADS1*, affects floral morphological features. Floral growth during later developmental stages may be stopped by silencing *PeMADS7*, *PeHB*, and *PeZIP*. In addition, co-silencing B- and C-class MADS-box genes revealed the importance of studying lip morphogenesis in orchid flowers, which cannot be addressed using model plants such as rice and *Arabidopsis*.

Supplementary material

Supplementary data are available at *JXB* online.

Supplementary Table S1. Primers for semi-quantitative RT-PCR and real-time RT-PCR amplification.

Supplementary Table S2. Ratios of features of plant organs affected by transcription-factor silencing.

Supplementary Table S3. Ratios of features of plant organs affected by transcription-factor silencing in three cultivars.

Supplementary Fig. S1. Effect of gene fragment length on successful insertion into the pCymMV-Gateway vector.

Supplementary Fig. S2. Analysis of *PeMADS7*, *PebZIP*, *PeHB*, *PeMADS1*, *PeMADS6*, *PebHLH* expression during flower development and in different tissues in *Phalaenopsis*.

Supplementary Fig. S3. Severity of floral organ morphological changes in *PeMADS1*-, *PeMADS6*-, and double-silenced flowers.

Supplementary Fig. S4. VIGS phenotypes of *PeMADS1*- and *PebHLH*-silenced plants in *Doritaenopsis* OX Red Shoe 'OX1407'.

Supplementary Fig. S5. The multiple sequence alignment of homeobox (HB) transcription factor nucleotide sequences from OrchidBase 2.0.

Supplementary Fig. S6. Phylogenetic analysis of *PebHLH* in *bHLH* gene families of *Arabidopsis* and rice.

Supplementary Fig. S7. Concurrent silencing of both *PeMADS1* and *PeMADS6* with a pCymMV-Gateway vector in *Doritaenopsis* OX Red Shoe 'OX1407'.

Supplementary Fig. S8. Concurrent silencing of both *PeMADS1* and *PeMADS6* with a pCymMV-Gateway vector in *Phalaenopsis* Sogo Yukidian 'V3'.

Supplementary Fig. S9. Cyro-SEM micrograph of epidermal cell arrangements of floral organs.

Supplementary Fig. S10. Cyro-SEM micrograph top and side view of adaxial and abaxial epidermal cells of *PeMADS1* and *PeMADS6* double-silenced floral organs from the first blooming flowers.

Supplementary Fig. S11. Estimation of the period of floral development is most sensitive to loss of function by *PeMADS1* and *PeMADS6* silencing in orchid.

Acknowledgements

The authors are grateful to Dr Wen-Chieh Tsai [Institute of Tropical Plant Science, National Cheng Kung University (ITPS, NCKU)] and Dr Chi-Kuang Wen (Institute of Plant Physiology and Ecology, Shanghai Institutes for Biological Sciences, Chinese Academy of Sciences) for helpful discussion of this work. The authors thank Dr Wann-Neng Jane (Plant Cell Biology Core Facility, Institute of Plant and Microbial Biology, Academia Sinica) for assisting with cryo-SEM of floral micro-structures. The authors thank Ms Jui-Ling Hsu (ITPS, NCKU) for assistance in agro-infiltration and real-time quantitative RT-PCR. The authors also thank Oxen Biotechnology (Tainan, Taiwan) for assistance in choosing plant materials.

References

Aida R, Murai K, Kishimoto S, Ohmiya A. 2003. Introduction of *WAG*, a wheat *AGAMOUS* homolog, reduces corolla size in torenia. *Bulletin of the National Institute of Floricultural Science* **3,** 21–27.

Becker A, Theissen G. 2003. The major clades of MADS-box genes and their role in the development and evolution of flowering plants. *Molecular Phylogenetics and Evolution* **29,** 464–489.

Bercu R, Bavaru A, Broasca L. 2011. Anatomical aspects of *Phalaenopsis amabilis* (L.) Blume. *Annals of the Romanian Society for Cell Biology* **16,** 102–109.

Bernacki S, Karimi M, Hilson P, Robertson N. 2010. Virus-induced gene silencing as a reverse genetics tool to study gene function. *Methods in Molecular Biology* **655,** 27–45.

Bowman JL, Smyth DR, Meyerowitz EM. 1989. Genes directing flower development in *Arabidopsis*. *The Plant Cell* **1,** 37–52.

Bowman JL, Smyth DR, Meyerowitz EM. 1991. Genetic interactions among floral homeotic genes of *Arabidopsis*. *Development* **112,** 1–20.

Bradley D, Carpenter R, Sommer H, Hartley N, Coen E. 1993. Complementary floral homeotic phenotypes result from opposite orientations of a transposon at the plena locus of *Antirrhinum*. *Cell* **72,** 85–95.

Chang YY, Kao NH, Li JY, Hsu WH, Liang YL, Wu JW, Yang CH. 2010. Characterization of the possible roles for B class MADS box genes in regulation of perianth formation in orchid. *Plant Physiology* **152,** 837–853.

Chen WH, Hsu CY, Cheng HY, Chang H, Chen HH, Ger MJ. 2011. Downregulation of putative UDP-glucose: flavonoid 3-*O*-glucosyltransferase gene alters flower coloring in *Phalaenopsis*. *Plant Cell Reports* **30,** 1007–1017.

Chen YH, Tsai YJ, Huang JZ, Chen FC. 2005. Transcription analysis of peloric mutants of *Phalaenopsis* orchids derived from tissue culture. *Cell Research* **15,** 639–657.

Chen YY, Lee PF, Hsiao YY, Wu WL, Pan ZJ, Lee YI, Liu KW, Chen LJ, Liu ZJ, Tsai WC. 2012. C- and D-class MADS-box genes from *Phalaenopsis equestris* (Orchidaceae) display functions in gynostemium and ovule development. *Plant and Cell Physiology* **53,** 1053–1067.

Chugh S, Guha S, Rao IU. 2009. Micropropagation of orchids: A review on the potential of different explants. *Scientia Horticulturae* **122,** 507–520.

Coen ES, Meyerowitz EM. 1991. The war of the whorls: genetic interactions controlling flower development. *Nature* **353,** 31–37.

Deng X, Xiong L, Wang Y, Li X. 2011. Ectopic expression of an *AGAMOUS* homolog *NTAG1* from Chinese narcissus accelerated earlier flowering and senescence in *Arabidopsis*. *Molecular Plant Breeding* **2,** 14–21.

Dressler RL. 2005. How many orchid species? *Selbyana* **26,** 155–158.

Fu CH, Chen YW, Hsiao YY, Pan ZJ, Liu ZJ, Huang YM, Tsai WC, Chen HH. 2011. OrchidBase: a collection of sequences of the transcriptome derived from orchids. *Plant and Cell Physiology* **52,** 238–243.

Geuten K, Irish V. 2010. Hidden variability of floral homeotic B genes in *Solanaceae* provides a molecular basis for the evolution of novel functions. *The Plant Cell* **22,** 2562–2578.

Heisler MGB, Atkinson A, Bylstra YH, Walsh R, Smyth DR. 2001. *SPATULA*, a gene that controls development of carpel margin tissues in *Arabidopsis*, encodes a bHLH protein. *Development* **128,** 1089–1098.

Hsiao YY, Pan ZJ, Hsu CC, Yang YP, Hsu YC, Chuang YC, Shih HH, Chen WH, Tsai WC, Chen HH. 2011. Research on orchid biology and biotechnology. *Plant and Cell Physiology* **52,** 1467–1486.

Hsiao YY, Tsai WC, Kuoh CS, Huang TH, Wang HC, Wu TS, Leu YL, Chen WH, Chen HH. 2006. Comparison of transcripts in *Phalaenopsis bellina* and *Phalaenopsis equestris* (Orchidaceae) flowers to deduce monoterpene biosynthesis pathway. *BMC Plant Biology* **6,** 14.

Hsieh MH, Lu HC, Pan ZJ, Yeh HH, Wang SS, Chen WH, Chen HH. 2013. Optimizing virus-induced gene silencing efficiency with *Cymbidium* mosaic virus in *Phalaenopsis* flower. *Plant Science* **201,** 25–41.

Ichihashi Y, Horiguchi G, Gleissberg S, Tsukaya H. 2010. The *bHLH* transcription factor *SPATULA* controls final leaf size in *Arabidopsis thaliana*. *Plant and Cell Physiology* **51,** 252–261.

Ikeda M, Mitsuda N, Ohme-Takagi M. 2013. ATBS1 INTERACTING FACTORs negatively regulate *Arabidopsis* cell elongation in the triantagonistic bHLH system. *Plant Signaling and Behavior* **8,** e23448.

Kapoor M, Tsuda S, Tanaka Y, Mayama T, Okuyama Y, Tsuchimoto S, Takatsuji H. 2002. Role of petunia *pMADS3* in determination of floral organ and meristem identity, as revealed by its loss of function. *The Plant Journal* **32,** 115–127.

Koch K, Bhushan B, Barthlott W. 2008. Diversity of structure, morphology and wetting of plant surfaces. *Royal Society of Chemistry* **10,** 1943–1963.

Kramer EM, Hodges SA. 2010. *Aquilegia* as a model system for the evolution and ecology of petals. *Philosophical Transactions of the Royal Society B* **365,** 477–490.

Ku SM, Kono Y, Liu Y. 2008. *Begonia pengii* (sect. *Coelocentrum*, Begoniaceae), a new species from limestone areas in Guangxi, China. *Botanical Studies* **49,** 167–175.

Li X, Duan X, Jiang H, *et al.* 2006. Genome-wide analysis of *basic/helix–loop–helix* transcription factor family in rice and *Arabidopsis*. *Plant Physiology* **141,** 1167–1184.

Liu X, Zuo K, Zhang F, Li Y, Xu J, Zhang L, Sun X, Tang K. 2009. Identification and expression profile of GbAGL2, a C-class gene from *Gossypium barbadense*. *Journal of Biosciences* **34,** 941–951.

Lu HC, Chen HH, Tsai WC, Chen WH, Su HJ, Chang DC, Yeh HH. 2007. Strategies for functional validation of genes involved in reproductive stages of orchids. *Plant Physiology* **143,** 558–569.

Lu HC, Hsieh MH, Chen CE, Chen HH, Wang HI, Yeh HH. 2012. A high-throughput virus-induced gene-silencing vector for screening transcription factors in virus-induced plant defense response in orchid. *Molecular Plant–Microbe Interactions* **25,** 738–746.

Meyerowitz EM, Bowman JL, Brockman LL, Drews GN, Jack T, Sieburth LE, Weigel D. 1991. A genetic and molecular model for flower development in *Arabidopsis thaliana*. *Development Supplement* **1,** 157–167.

Pan ZJ, Cheng CC, Tsai WC, Chung MC, Chen WH, Hu JM, Chen HH. 2011. The duplicated B-class MADS-box genes display dualistic characters in orchid floral organ identity and growth. *Plant and Cell Physiology* **52,** 1515–1531.

Pires N, Dolan L. 2010. Origin and diversification of basic-helix–loop–helix proteins in plants. *Molecular Biology and Evolution* **27,** 862–874.

Pnueli L, Hareven D, Rounsley SD, Yanofsky MF. 1994. Isolation of the tomato *AGAMOUS* gene *TAG7* and analysis of its homeotic role in transgenic plants. *American Society of Plant Physiologists* **6,** 163–173.

Prüm B, Seide, I.R, Bohn HF, Speck T. 2012. Impact of cell shape in hierarchically structured plant surfaces on the attachment of male Colorado potato beetles (*Leptinotarsa decemlineata*). *Beilstein Journal of Nanotechnology* **3,** 57–64.

Song IJ, Nakamura T, Fukuda T, Yokoyama J, Ito T, Ichikawa H, Horikawa Y, Kameya T, Kanno A. 2006. Spatiotemporal expression of duplicate *AGAMOUS* orthologues during floral development in *Phalaenopsis*. *Development Genes and Evolution* **216,** 301–313.

Szecsi J, Joly C, Bordji K, Varaud E, Cock JM, Dumas C, Bendahmane M. 2006. *BIGPETALp*, a *bHLH* transcription factor is involved in the control of *Arabidopsis* petal size. *The EMBO Journal* **25,** 3912–3920.

Tsai WC, Fu CH, Hsiao YY, Huang YM, Chen LJ, Wang M, Liu ZJ, Chen HH. 2013. OrchidBase 2.0: comprehensive collection of Orchidaceae floral transcriptomes. *Plant and Cell Physiology* **54,** e7.

Tsai WC, Hsiao YY, Lee SH, Tung CW, Wang DP, Wang HC, Chen WH, Chen HH. 2006. Expression analysis of the ESTs derived from the flower buds of *Phalaenopsis equestris*. *Plant Science* **170,** 426–432.

Tsai WC, Hsiao YY, Pan ZJ, Chen HH. 2010. Molecular mechanisms underlying orchid floral morphogenesis. *Acta Horticulturae* **878,** 115–123.

Tsai WC, Lee PF, Chen HI, Hsiao YY, Wei WJ, Pan ZJ, Chuang MH, Kuoh CS, Chen WH, Chen HH. 2005. *PeMADS6*, a *GLOBOSA*/*PISTILLATA*-like gene in *Phalaenopsis equestris* involved in petaloid formation, and correlated with flower longevity and ovary development. *Plant and Cell Physiology* **46,** 1125–1139.

Tsai WC, Pan ZJ, Hsiao YY, Jeng MF, Wu TF, Chen WH, Chen HH. 2008. Interactions of B-class complex proteins involved in tepal development in *Phalaenopsis* orchid. *Plant and Cell Physiology* **49,** 814–824.

Vandenbussche M, Zethof J, Royaert S, Weterings K, Gerats T. 2004. The duplicated B-class heterodimer model: whorl-specific effects and complex genetic interactions in *Petunia hybrida* flower development. *The Plant Cell* **16,** 741–754.

Varaud E, Brioudes F, Szecsi J, Leroux J, Brown S, Perrot-Rechenmann C, Bendahmane M. 2011. *AUXIN RESPONSE FACTOR8* regulates *Arabidopsis* petal growth by interacting with the *bHLH* transcription factor *BIGPETALp*. *The Plant Cell* **23,** 973–983.

Wang H, Zhu Y, Fujioka S, Asami T, Li J. 2009. Regulation of *Arabidopsis* brassinosteroid signaling by atypical basic helix–loop–helix proteins. *The Plant Cell* **21,** 3781–3791.

Whitney HM, Bennett KM, Dorling M, Sandbach L, Prince D, Chittka L, Glover BJ. 2011. Why do so many petals have conical epidermal cells? *Annals of Botany* **108,** 609–616.

Xu Y, Teo LL, Zhou J, Kumar PP, Yu H. 2006. Floral organ identity genes in the orchid *Dendrobium crumenatum*. *The Plant Journal* **46,** 54–68.

Xu Y, Yu H, Kumar PP. 2010. Characterization of floral organ identity genes of the orchid *Dendrobium crumenatum*. *Asia-Pacific Journal of Molecular Biology and Biotechnology* **18,** 185–187.

Yamaguchi T, Lee DY, Miyao A, Hirochika H, An G, Hirano HY. 2006. Functional diversification of the two C-class MADS box genes *OSMADS3* and *OSMADS58* in *Oryza sativa*. *The Plant Cell* **18,** 15–28.

Yanofsky MF, Ma H, Bowman JL, Drews GN, Feldmann KA, Meyerowitz EM. 1990. The protein encoded by the *Arabidopsis* homeotic gene agamous resembles transcription factors. *Nature* **346,** 35–39.

Yun D, Liang W, Dreni L, Yin C, Zhou Z, Kater MM, Zhang D. 2013. *OsMADS16* genetically interacts with *OsMADS3* and *OsMADS58* in specifying floral patterning in rice. *Molecular Plant* **6,** 743–756.

Zachgo S, de Andrade Silva E, Motte P, Tröbner W, Saedler H, Schwarz-Sommer Z. 1995. Functional analysis of the *Antirrhinum* floral homeotic *DEFICIENS* gene *in vivo* and *in vitro* by using a temperature-sensitive mutant. *Development* **121,** 2861–2875.